Drop Formation Mechanism in a Vertically Vibrated Liquid Column

H. Hashimoto* and S. Sudo†
Tohoku University, Sendai, Japan

The purpose of the present paper is to clarify the hydrodynamical mechanism of surface disintegration and drop formation over a wide range of input frequency and amplitude. The experiment involved longitudinal excitation of a container of water on an electrodynamic shaker. The free surface behavior in the vibrating container was analyzed by using a 16-mm high-speed camera and an automatic liquid surface detector. The threshold of surface disintegration and the wave characteristics of large-amplitude surface motions with liquid drops in a vertically excited rectangular container have been investigated experimentally. The drop formation mechanism and the drop size distribution have also been examined, both theoretically and experimentally. The results obtained here should provide useful clues for future research and development of application fields of the liquid sloshing phenomena.

Nomenclature

C = compliance
D = drop diameter
E = amplitude
F = force
f = frequency
g = gravitational acceleration
G = dimensionless acceleration, $G = (2\pi f_0)^2 E_0/g$
h = liquid height
I_0, I_1 = modified Bessel function
k = dimensionless wave number
L = length of liquid column
N = percentage rate of drop number
N' = drop number per unit time
r = dimensionless radius coordinate
R = liquid column radius
t = time
T = period of liquid surface motion
X_L = total amplitude of liquid surface motion
W = width of container
z = dimensionless axis coordinate
η = dimensionless surface displacement
σ = surface tension
ϕ = velocity potential
ω = angular velocity

Subscripts

d = liquid drop
0 = input

Introduction

THE importance of the study of the dynamic behavior of liquid in a moving container is well recognized. Many studies on this subject have been done for the instability problem of liquid fuel rockets, the seismic design of liquid storage tanks, safety-related liquids in nuclear plants, and the mixing process of gas and liquid in chemical engineering. Currently, a more detailed investigation on the liquid surface behavior is required in order to make effective use of the liquid sloshing characteristics at high input acceleration in these engineering fields.

Studies of the liquid surface behavior in vertically vibrating containers at high input acceleration include investigation of the 1/2-subharmonic wave response of the input frequency,[1] liquid surface disintegration at a high frequency,[2] pressure distribution and bubble formation,[3] liquid drop ejection and gas entrainment from the free surface,[4] violent surface agitation by gas injection,[5] and frequency characteristics of a bubble cluster.[6] Large-amplitude motions, such as hyperbolic jets[7] or steep nonlinear waves[8] according to the free surface wave growth in the field of gravity and surface tension, have also been analyzed. Several studies on drop formation with respect to the atomization of the liquid jet[9] have also been reported. However, the relationship of the input conditions to the characteristics of the surface wave with liquid drops has not been clarified in detail. In particular, further investigation into the mechanism of surface disintegration in the liquid sloshing is required because the liquid interface at the high input acceleration presents very complicated behavior accompanying surface disintegration and because research data on drop formation are insufficient and many unexplored problems still remain. A fundamental investigation of a means of systematizing such complicated phenomena is also important.

The purpose of the present paper is to clarify hydrodynamically the mechanism of surface disintegration and drop formation over a wide range of input frequency and amplitude. The wave characteristics of large-amplitude surface motions with liquid drops in a vertically excited rectangular container have been investigated experimentally. The drop formation mechanism and the drop size distribution have also been examined, both theoretically and experimentally. The results obtained here should provide useful clues for future research and development of the above-mentioned liquid sloshing field.

Experimental Apparatus and Procedures

A block diagram of a vibration exciter and a measuring system is shown in Fig. 1. An electrodynamic shaker was operated at a given frequency, displacement, and acceleration.[4] A square rectangular container (300 mm long, 50 mm × 50 mm wide, 5 mm deep) was made of transparent acrylic to allow optical observation. Tap water at approximate 17°C was used as the test liquid.

The experiment involved the longitudinal excitation of the container of water on the electrodynamic shaker. The liquid tank system was usually excited at a constant frequency so that the amplitude (i.e., the acceleration) would begin to

Received March 5, 1986; revision received Aug. 5, 1986.

*Professor, Institute of High Speed Mechanics. Member AIAA.
†Research Assistant, Institute of High Speed Mechanics.

increase gradually from zero amplitude. Several piezoelectric accelerometers, together with charge amplifiers, were used to measure the vibration components of the container. The free surface behavior in the vibrating container was analyzed by using a 16-mm high-speed camera and a film motion analyzer. The displacement of the liquid free surface was also measured by an optical cathetometer. Measurement of large-amplitude surface motions with liquid drops was also made with an automatic liquid surface detector. The signals from the detector were analyzed by a fast Fourier transform (FFT) analyzer.

Experimental Results and Discussion

Surface Disintegration

As the input acceleration or the excitation acceleration increased slowly at a given frequency, a wave appeared on the liquid free surface. Such a surface response is usually referred to as a 1/2-subharmonic response, as the exciting frequency of the container is two times the liquid surface frequency. Further increase in excitation acceleration caused the crests of the 1/2-subharmonic wave to disintegrate and form liquid spray. The results of the surface disintegration for several water heights in the rectangular container are shown in Fig. 2. Figure 2 shows the relation of the input frequency f_0 and the input dimensionless acceleration G_0 $(G_0 = (2\pi f_0)^2 E_0/g)$ at the beginning of the surface disintegration. The dimensionless acceleration required to disintegrate the liquid surface (threshold spray) varies linearly with the input frequency for the lower frequencies. The effects of water height are very apparent in the higher frequencies; the greater the water height, the less the threshold input acceleration. This trend is similar to the case of the cylindrical container.[4] Thus, there seems to be a tendency that it is not influenced by individual container shapes if the container scale is much larger than the wavelength of the surface wave.

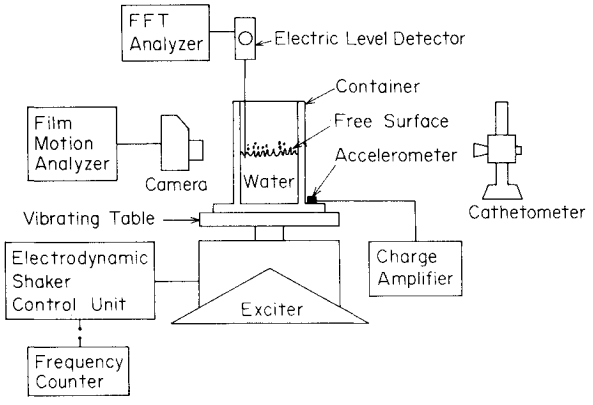

Fig. 1 Block diagram of experimental apparatus.

Amplitude of Surface Motion with Drops

By increasing the input acceleration above the threshold input acceleration, the surface accompanying small drops oscillated with a lower mode and possibly a large amplitude. Research data on the lower mode wave, the spray-excited wave, are insufficient, and a large part still remains unexplored. In order to obtain more fundamental knowledge, the following measurements of this wave were made. The total amplitude X_L, the sum of the maximum rise and the maximum depression of the liquid surface in a container, was measured at the representative position, which was 5 mm away from two walls at a corner of the container. As the input acceleration increased at a given constant frequency, the amplitude X_L of the surface motion with liquid drops increased. Figure 3 shows the relation between the dimensionless total amplitude X_L/W and the dimensionless input acceleration G_0 for a water height $h/W = 3.0$. The chain line in the figure shows the threshold of spray. It can be seen from Fig. 3 that X_L/W increases with G_0 at the constant input frequency f_0 and increases with f_0 at the constant G_0 within the range of the measurement. This trend is similar to the case of the cylindrical container.[4] No special difference between both containers is recognized regarding the relation of X_L to G_0.

Compliance of Surface Response

The compliance C is defined by the input force F and the amplitude X_L measured at the above-mentioned representative position, i.e., $C = X_L/(2F)$. Figure 4 shows the relation between the compliance C and the excitation acceleration G_0 for the water height $h/W = 2.0$. The compliance C depends on the excitation frequency f_0 and the excitation amplitude E_0 proportional to G_0, and C has a minimum. The larger f_0 is, the smaller C is. A similar trend was conformed in the other water height. Figure 5 shows schematically the correspondence of C to the behavior of the liquid free surface. The liquid surface disintegrated at the G_a point and presented the large-amplitude spray-excited mode at the G_b point. In the region $G_0 < G_a$, the free surface presents the 1/2-subharmonic response. In this region, C decreases with the rise of G_0. Thus, the amplitude of the 1/2-subharmonic wave does not become very large, even if G_0 increases. In the region $G_a < G_0 < G_b$, the amplitude of the surface with the disintegration became large gradually. The difference between the value G_a and G_b became small rapidly with the rise of f_0, and G_a approxi-

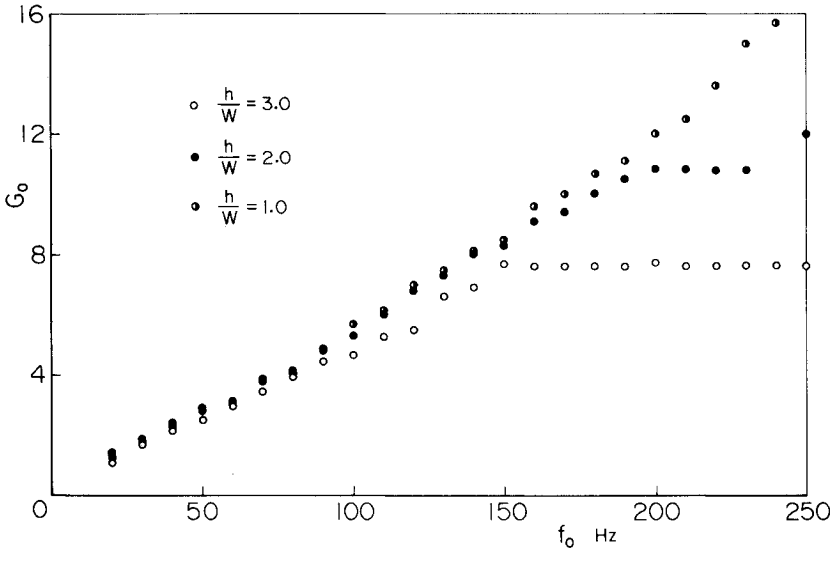

Fig. 2 Relation of dimensionless input acceleration G_0 to frequency f_0 for threshold spray.

mately coincided with G_b if the frequency was above 80 Hz. In the region $G_0 > G_b$, C increases with the rise of G_0. This is caused by the occurrence of large-amplitude spray-excited waves with much lower frequencies than f_0, so that the amplitudes increase steeply with a rise of G_0, as shown in Fig. 3. As described above, this compliance-excitation acceleration curve is a convenient means of understanding the relation of the dynamic behavior of a liquid free surface to the input conditions.

Period of Surface Motion

When the surface didn't disintegrate, the period of the surface motion was two times the input period independently of the input acceleration; the liquid free surface always presented a 1/2-subharmonic response. But when the surface disintegrated and the large-amplitude free surface motions with spray drops occurred, the period T of the spray-excited wave varied with the input acceleration. Figure 6 shows the relation between T and G_0 at $h/W = 2.0$ and $h/W = 3.0$. The lower f_0 is, the larger is the increasing rate of T. T increases with G_0, but the period is scarcely influenced by the height h/W. The upper limiting value of the spray-excited wave period was 0.25 ~ 0.26 s. This limiting period was different from the period of the cylindrical container; it seems to take a unique value for each container. The input acceleration required for the occurrence of the limiting period motion increased with the input frequency.

The free surface of each spray-excited surface wave with many drops was composed of the low-frequency, large-amplitude wave and the small-amplitude subharmonic waves. The wavelength of the subharmonic wave was very small compared with that of the large-amplitude wave. The most drops were formed from the subharmonic waves superimposed on the large-amplitude wave. The spray-excited surface motions were traced by the automatic liquid surface detector, which utilized a surbomotor system, and the signals were analyzed by the FFT analyzer. This detector traces approximately only the low-frequency, large-amplitude wave because the amplitude of the subharmonic wave is too small and the frequency too high to be sensed by the detector. As a representative example, the results of tests on time and frequency domains are shown in Fig. 7. It can be seen from the figure that the liquid free surface responds as a relatively regular spray-excited wave having little deviations in its frequency and amplitude; the signal $X_L(t)$ on a time scale shows an almost regular sinusoidal wave and has a remarkable peak in the frequency spectrum $|X_L(f)|$.

As described above, the distinctive characteristics of the spray-excited wave were clarified in detail, and it clearly differed from the well-known characteristics of 1/2-subharmonic waves.

Liquid Drop Size

Figure 8 shows the representative drop size spectra at $h/W = 2.0$. In Fig. 8, the abscissa shows the dimensionless drop diameter D/W, and the ordinate shows the number N of the drop in a percentage value. It can be seen that the

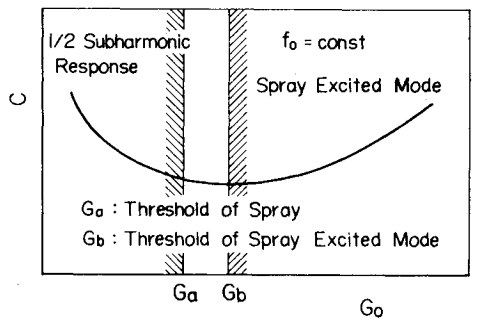

Fig. 5 Schematic compliance curve and surface response.

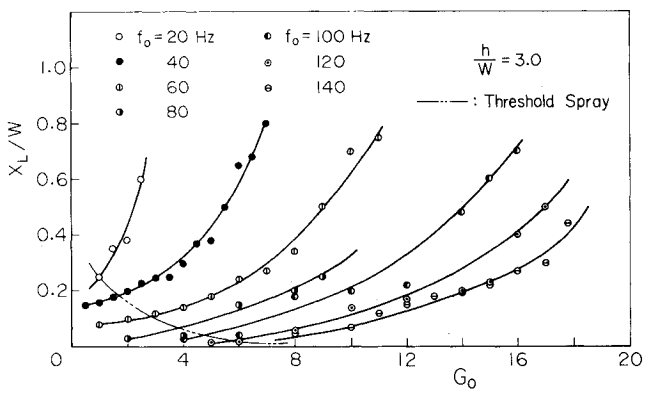

Fig. 3 Relation between the dimensionless total amplitude and input acceleration G_0 for $h/W = 3.0$.

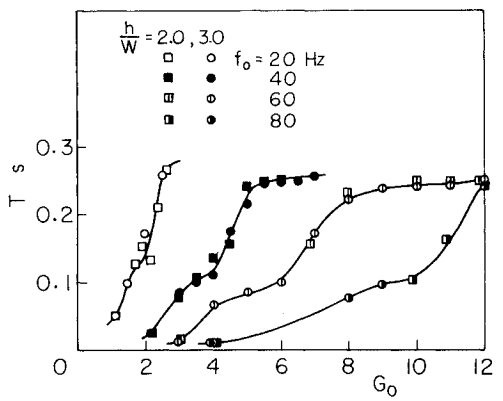

Fig. 6 Relation between period and acceleration for $h/W = 2.0$ and $h/W = 3.0$.

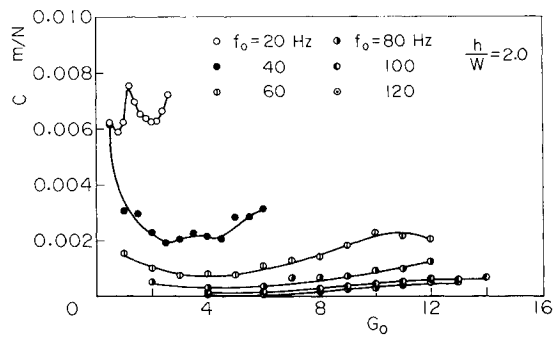

Fig. 4 Relation of compliance C to G_0 for $h/W = 3.0$.

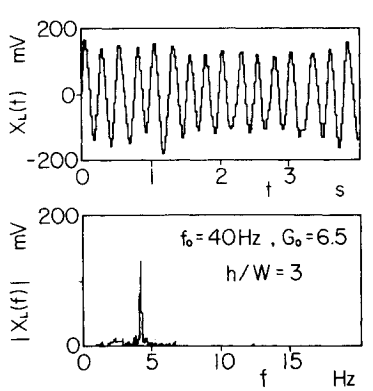

Fig. 7 Example of measuring results of surface wave amplitude.

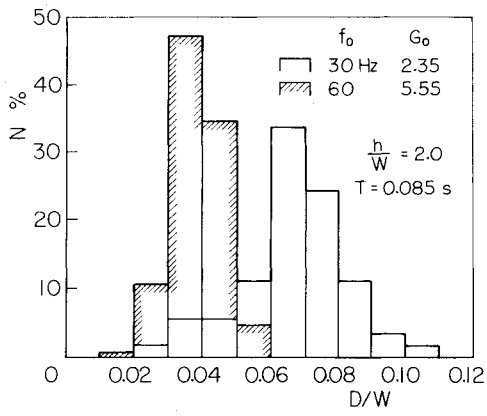

Fig. 8 Drop size spectra for $h/W = 2.0$, $f_0 = 30$ Hz and $f_0 = 60$ Hz.

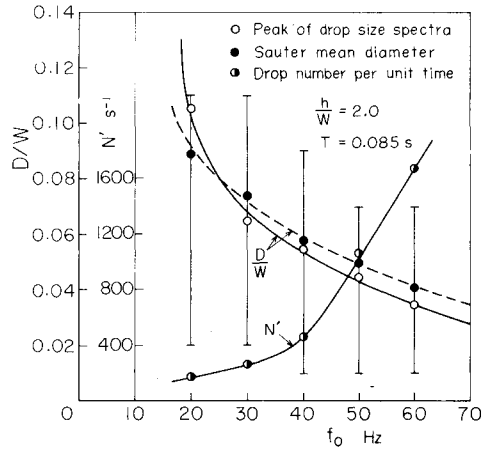

Fig. 9 Relation of f_0 to drop size.

distribution of drop sizes expands relatively. Figure 9 shows the relation of the input frequency to the dimensionless drop size. In the figure, ○ and ● indicate the peak drop size distribution and the Sauter mean diameter, respectively, and the upper and lower limits are indicated by a short solid line. It can be seen from Figs. 8 and 9 that the mean value of the dimensionless drop diameter decreases gradually with a rise of f_0 and that the expansion of drop size distribution narrows a little with a rise of f_0. Figure 9 also shows the number N' of liquid drops ejected from the free surface per unit time. As the input frequency increases, the number of drops increases rapidly. This is because the wave number of 1/2-subharmonic waves superimposed on the slow, large-amplitude wave in the container increases with a rise in the input frequency.

Mechanism of Drop Formation

The liquid disintegration of the free surface was observed by a high-speed camera. The growth rate of the top part of the liquid column was very large compared to the horizontal width of the column; that is, cylindrical jet columns were formed on the liquid surface. A swell appeared immediately at the top of the liquid jet. Subsequently, a neck appeared just below the swell, and the swell grew rapidly. Finally, the liquid column disintegrated into a liquid droplet at the neck point, as shown in Fig. 10. Sometimes a few necks appeared along the column, and then a few droplets were generated at one time. The time interval between frames in Fig. 10 is 0.008 s. A similar disintegration pattern was observed for the other input frequencies. The results, as shown by a film motion analyzer at $f_0 = 20$ Hz and at $f_0 = 40$ Hz, are shown in Figs. 11 and 12, respectively. The dimensionless vertical height from the stationary level and the swell and the neck of the liquid column

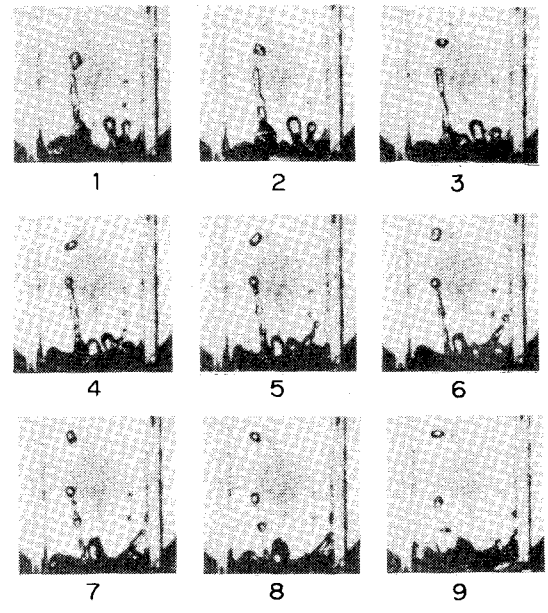

Fig. 10 Real-time sequence photographs of drop formation.

are plotted vs the time sequence in the figure. It can be seen from the figure that the vertical height of the liquid column formed by the growth of 1/2-subharmonic wave rapidly becomes large with time.

The drop formation can be considered theoretically as follows. In general, the free interface between gas and liquid becomes unstable and the liquid column grows when the applied acceleration to the interface is directed from the heavier liquid and lighter fluid. In the following analysis, only one liquid column is considered among others in order to simplify understanding of the phenomena. It is assumed that the fluid is nonviscous and incompressible and that it is restricted to a short time duration required for a drop formation from the liquid column. The growth velocity of the liquid column is assumed to be constant approximately within this short time. From the experiment, the initial geometrical form of the liquid column can be assumed to be a smooth axisymmetric circular cylinder with uniform radius R, and the axial length of the liquid column to be long enough compared with R.

A cylindrical dimensionless coordinate system (r, z) is used. The z axis corresponds to the centerline of the liquid column, and the plane $z = 0$ corresponds to the liquid free surface. All physical values are expressed in the dimensionless form by characteristic length R, time $(\rho R^3/\sigma)^{1/2}$, velocity $(\sigma/R\rho)^{1/2}$, and pressure σ/R, where σ and ρ are the fluid surface tension and density, respectively. The dimensionless velocity potential ϕ satisfies Laplace's equation:

$$\nabla^2\phi = 0 \tag{1}$$

The kinematic and dynamic boundary conditions are expressed in the following equations:

$$\left[\frac{\partial}{\partial t} + (\nabla\phi\cdot\nabla)\right]\eta = \frac{\partial\phi}{\partial r} \tag{2}$$

$$\frac{\partial\phi}{\partial t} + \frac{1}{2}\left[\left(\frac{\partial\phi}{\partial r}\right)^2 + \left(\frac{\partial\phi}{\partial z}\right)^2\right] = \frac{\partial^2\eta}{\partial z^2}\Big/\left[1+\left(\frac{\partial\eta}{\partial z}\right)^2\right]^{3/2} - 1/(1+\eta)\sqrt{1+\left(\frac{\partial\eta}{\partial z}\right)^2} + 1 \tag{3}$$

on the surface

$$r = 1 + \eta(z,t)$$

where $\eta(z,t)$ is the dimensionless surface wave amplitude. The following equations are introduced from the initial conditions that the liquid volume at $t=0$ along the surface $\eta = \eta_0 \cos(kz)$ equals the standard static volume with $r=1$ and initial radial velocity $\eta_t = 0$:

$$\eta(z,0) = \eta_0 \cos(kz) + \left(1 - 1/2\eta_0^2\right)^{1/2} - 1 \tag{4}$$

$$\eta_t(z,0) = 0 \tag{5}$$

These equations were analyzed as a nonlinear problem of a liquid jet.[10] In this paper, the analytical method of Lafrance[11] was applied with the assumption that the fluid was water and the motion of the surrounding gas flow was negligible. We consider that the surface disturbance and the velocity potential can be expressed in the following perturbation series in terms of the small parameter η_0:

$$\eta(z,t) = \sum_{n=1}^{\infty} \eta_0^n \eta_n(z,t) \tag{6}$$

$$\phi(r,z,t) = \sum_{n=1}^{\infty} \eta_0^n \phi_n(r,z,t) \tag{7}$$

The first-order solution obtained by substituting these two equations into the above fundamental equations is identical to the simple solution by Rayleigh:

$$\eta_1 = \cosh(\omega_1 t)\cos(kz) \tag{8}$$

$$\phi_1 = \frac{\omega_1}{k}\frac{I_0(kr)}{I_1(k)}\sinh(\omega_1 t)\cos(kz) \tag{9}$$

where I_0 and I_1 are the modified Bessel functions of the zeroth and first order, respectively, and parameter ω_1 is expressed in the following equation:

$$\omega_1^2 = \frac{k(1-k^2)}{I_a}, \quad I_a = \frac{I_0(k)}{I_1(k)}$$

The second-order solutions $\eta_2(z,t)$ and $\phi_2(r,z,t)$ and the third-order solutions $\eta_3(z,t)$ and $\phi_3(r,z,t)$ are obtained in the same way as the first-order solutions. In the numerical analysis, we took the third-order solution into consideration.

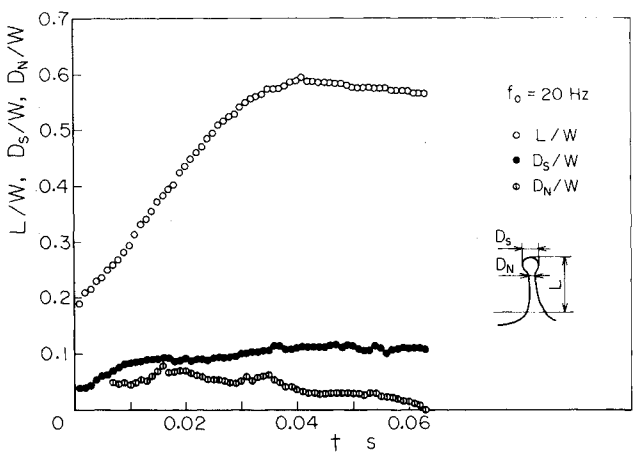

Fig. 11 Liquid column deformation and drop formation for f_0 = 20 Hz.

Figure 13 is a representative example of the results for the initial condition $k = 0.3$. The figure shows that if unstable axisymmetric disturbances occur on the surface of the vertical liquid column, the amplitude of the unstable disturbance wave increases rapidly and nonuniformly with time. It can be seen from the calculated result that there is a possibility that smaller drops as well as the main large drops will be formed. Thus, it can be expected that the drop size distributions are expanded by these small drops. The patterns of the drop formation, as observed by a high-speed camera, are shown in Fig. 10. Several drops observed on the free surface oscillated in various modes due to their kinetic and surface energy. The figure shows that there are drops that contain the smaller size drops, as shown in Fig. 8. This supports the validity of the theoretical analysis.

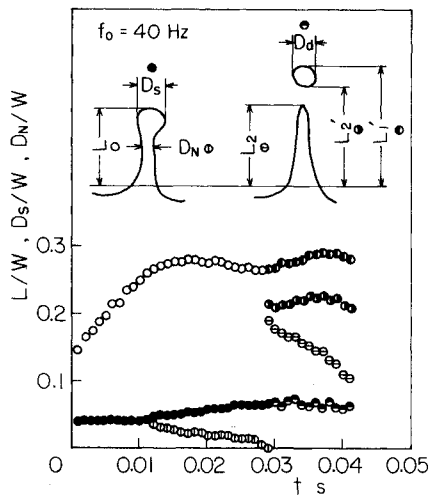

Fig. 12 Liquid column deformation and drop formation for f_0 = 40 Hz.

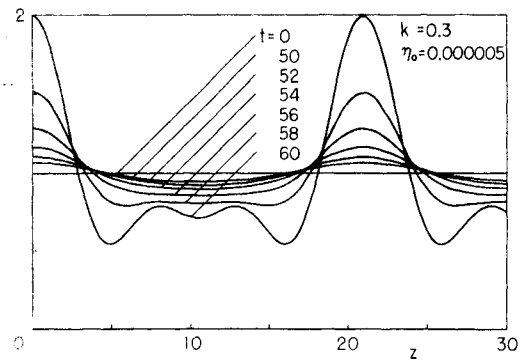

Fig. 13 Calculated amplitude of unstable surface wave.

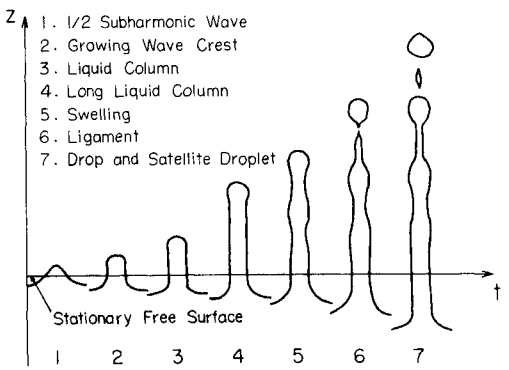

Fig. 14 Representative pattern of the surface disintegration.

The surface disintegration pattern investigated theoretically and experimentally is shown schematically in Fig. 14 (points $1 \sim 7$). The small 1/2-subharmonic waves are first generated on the plain free surface by the longitudinal vibration. This wave grows rapidly and forms a liquid column when the acceleration is directed from the liquid toward the air ($2 \sim 4$). Point 5 shows the swell and the neck on a liquid column, that is, the unstable waves generated on the vertical liquid column surface. The first drop formation is shown in point 6. The remaining liquid column becomes a fine ligament while the liquid drop leaves the liquid column. As shown in point 7, the ligament is cut off at the top of the second swell, and a solitary ligament is formed. The intermediate part of this ligament swells and deforms into a small liquid drop.

As described, the wave characteristics of the free surface with liquid drops and the mechanism of the drop formation were clarified by both experiment and theoretical analysis. These data should be useful for the improvement of the hydrodynamic machinery and apparatus accompanying the liquid sloshing.

Conclusions

The wave characteristics of the free surface accompanying liquid drops and the mechanism of drop formation in vertical vibration have been studied. The study indicated the following significant results:

The liquid free surface after the surface disintegration presents a relatively regular wave motion accompanying spray drops. In this surface response, the wave amplitude increases with a rise in the input frequency when the input acceleration is kept constant. The compliance increases with a rise in the input acceleration, and the period of this wave gradually approaches an upper limiting value ($T \simeq 0.26$) with a rise in the input acceleration.

In the general disintegration pattern, the 1/2-subharmonic wave grows with a rise in the input acceleration and becomes a cylindrical long liquid column with a round top. Unstable axisymmetric disturbances occur on the surface of the liquid column, and the swell and the neck near the top end of the column then appear as the amplitude of the disturbance becomes larger. Finally, as the liquid surface disintegrates, the drop is formed. When the input frequency increases, the mean drop size becomes smaller. The size spectra of drops ejected from a free surface have extending distributions.

The numerical result based on a weakly nonlinear theory also suggested that the formation of the small droplet was incidental to the main large drop formation.

References

[1]Dodge, F.T., Kana, D.D., and Abramson, H.N., "Liquid Surface Oscillations in Longitudinally Excited Rigid Cylindrical Containers," *AIAA Journal*, Vol. 3, April 1965, pp. 685–695.

[2]Gerlach, C.R., "Surface Disintegration of Liquid in Longitudinally Excited Containers," *Journal of Spacecraft and Rockets*, Vol. 5, May 1968, pp. 553–560.

[3]Shoenhals, R.J. and Overcamp, T.J., "Pressure Distribution and Bubble Formation Induced by Longitudinal Vibration of a Flexible Liquid-Filled Cylinder," *Transactions of the ASME*, Series D., Vol. 89, Dec. 1967, pp. 737–747.

[4]Hashimoto, H. and Sudo, S., "Surface Disintegration and Bubble Formation in Vertically Vibrated Liquid Column," *AIAA Journal*, Vol. 18, April 1980, pp. 442–449.

[5]Hashimoto, H. and Sudo, S., "Dynamic Behavior of Liquid Free Surface in a Cylindrical Container Subject to Vertical Vibration," *Bulletin of the JSME*, Vol. 2, May 1984, pp. 923–930.

[6]Hashimoto, H. and Sudo, S., "Frequency Characteristics of a Bubble Cluster in a Vibrated Liquid Column," *Journal of Spacecraft and Rockets*, Vol. 22, Dec. 1985, pp. 649–655.

[7]Longuet-Higgins, M.S., "Bubbles, Breaking Waves and Hyperbolic Jets at a Free Surface," *Journal of Fluid Mechanics*, Vol. 127, 1983, pp. 103–121.

[8]Hogan, J., "Particle Trajectories in Nonlinear Gravity-Capillary Waves," *Journal of Fluid Mechanics*, Vol. 151, 1985, pp. 105–119.

[9]Hertz, C.H. and Mermanrud, R., "A Liquid Compound Jet," *Journal of Fluid Mechanics*, Vol. 131, 1983, pp. 271–287.

[10]Nayfeh, A.H., "Nonlinear Stability of a Liquid Jet," *Physics of Fluids*, Vol. 13, April 1970, pp. 841–847.

[11]Lafrance, P., "Nonlinear Breakup of a Laminar Liquid Jet," *Physics of Fluids*, Vol. 18, April 1975, pp. 428–432.